

Stable biking control for manned bicycle with speed assistance

Keigo Kuriyama[†], Yuzuki Sugawara and Masami Iwase

Department of Robotics and Mechatronics, Tokyo Denki University, Tokyo, Japan
(E-mail: {kuriyama21,sugasawa20,iwase}@ctrl.fr.dendai.ac.jp)

Abstract: The objective of this research is to realize a posture stabilization control system that suppresses bicycle wobble, thereby reducing accidents caused by rider-induced unbalance. To achieve this goal, we first derive a dynamic model that accurately represents bicycle behavior. Based on this model, a speed-assist control system is designed to enable the bicycle to stably travel along a specified turning radius. The effectiveness of the proposed control system is then verified through experiments using the developed bicycle hardware.

Keywords: bicycle, stabilizing control, speed assistance

1. INTRODUCTION

Bicycles are widely used as a means of transportation across all age groups, and have become an integral part of daily mobility. Opportunities for bicycle use have increased through initiatives such as the provision of shared bicycles in tourist areas, expanding access to cycling even for those who do not own a bicycle [1, 2]. Bicycle-sharing systems have been adopted in cities around the world. One reason for this is that bicycles are considered environmentally friendly, as they do not rely on fossil fuels, making them a transportation option with a low environmental impact [3, 4]. For these reasons, bicycles are expected to become even more prevalent in the future.

However, bicycles are known to be unstable vehicles with a high risk of falling, and instability is influenced by speed, steering angle, and the tilt of the bicycle [5, 6]. One reason for this instability is that a bicycle is non-minimum phase and underactuated system. When the rider has poor balance or the bicycle's speed is outside the stable speed range, wobbling can occur, potentially leading to a fall [7].

To address the risks of the increasing number of accidents involving bicycle falling over, we propose that a control system capable of suppressing bicycle wobble could effectively reduce accidents. Yasuhito Tanaka, Toshiyuki Murakami, and colleagues proposed a dynamic model of the bicycle aimed at achieving posture stabilization. They designed a steering control method based on acceleration control and confirmed its effectiveness through both simulations and real-world experiments [8]. Additionally, Lychee Keo and Sirichai Pornsarayouth proposed a control algorithm that switches between flywheel and balancer modes to stabilize unmanned electric bicycles. They found that this approach improved stability performance and expanded the stable region compared to methods that relied solely on a balancer [9]. Furthermore, Pongsakorn Seekhao and colleagues aimed to stabilize the bicycle's posture using steering and pendulum motions. They applied linearization to a nonlinear model and LQR control, confirming the effectiveness of this approach in real-world applica-

tions [10].

However, most of these studies do not account for the dynamics of bicycles with human riders. In practice, when the rider's operation is inappropriate, the balance of the bicycle may be lost, potentially leading to a fall. Moreover, although posture stabilization is achieved through mechanisms such as motors attached to the steering, flywheels, and balance arms, bicycles equipped with such features are not commonly implemented in commercial products. In contrast, electrically-assisted bicycles that support the rider's pedaling operation have become widespread. Among the three factors related to bicycle wobbling, assisting vehicle speed is considered the most feasible, as the mechanism of electric assist bicycles can be repurposed for this function [11].

Therefore, this study investigates speed-assist control for scenarios in which a bicycle is turning and the rider's steering input becomes inappropriate for the bicycle's current conditions such as speed or incline. As a preliminary study, we derive a mathematical model that captures the dynamic behavior of a bicycle. Based on the model, we compute the speed required to maintain balance, i.e., equilibrium, while following a specified turning radius. To ensure stable riding even under simulated inappropriate steering conditions, a method is established in which the angular velocity in the roll direction is fed back to the bicycle's speed, allowing for acceleration or deceleration to improve riding stability. Through experiments on a real machine, the effect of angular velocity feedback in the roll direction on bicycle posture is evaluated.

2. BICYCLE MODEL DERIVATION

In this study, we derive a mathematical model of a bicycle based on the model proposed by Karl J. Åström. [12]. The bicycle model used is shown in Fig. 1, and the parameters of the model are listed in Table 1.

This model consists of four rigid bodies: the rear wheel, front wheel, rear frame, and steering. Each rigid body is assumed to be symmetric with respect to the bicycle's sagittal plane. The front and rear wheels are in contact with the ground, and the bicycle moves at a constant speed. The trail effect, which is one of the factors influencing the relationship between the bicycle's roll angle

[†] Keigo Kuriyama is the presenter of this paper.

Table 1 The independent variable

symbol	description
M	Mass of bicycle
m_f	Mass of front wheel
L	Wheel base
L_1	CoG position from rear wheel grounging point
L_2	CoG position from front wheel grounging point
L_3	Trail
h	CoG height
f	Fork offset
r_f	front Wheel radius
r_r	rear Wheel radius
λ	Caster angle
I_{xx}	Inertia of bicycle body about x axis
I_{xz}	Inertia of bicycle body about xz axis
I_h	Inertia of steering part
I_f	Inertia of front wheel part
I_r	Inertia of rear wheel part
ϕ	Roll angle
θ	steering angle
ψ	Turning round angle of bicycle body
V	Verocity of bicycle
ω	Rotary speed of wheel
τ_h	input torque
c	viscous friction
d	coulomb friction

and steering angle, is also taken into account. In deriving the equations of motion, the state vector q is defined as $q = [\dot{\phi} \ \dot{\theta} \ \phi \ \theta \ \psi]^T$.

When the bicycle is tilted with the handlebars turned, the contact point of the front wheel shifts. Let the amount

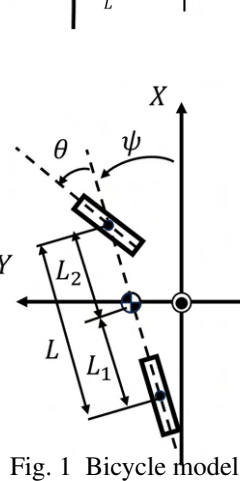
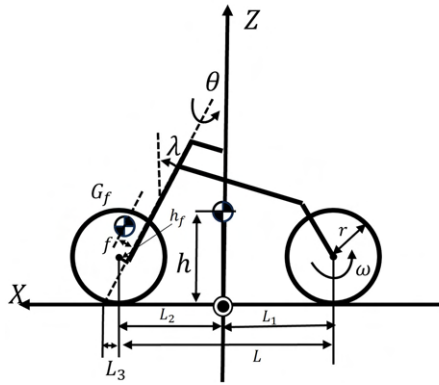


Fig. 1 Bicycle model

of this shift be denoted by δL_3 , and the distance to the new contact point after the shift be $\delta L'_3$; this situation is illustrated in Fig. 2. From Fig. 2, the shift in the contact point can be determined by Eq. (1);

$$\delta L_3 = r_f \sin \phi. \quad (1)$$

Therefore, the amount of trail after the change can be expressed by Eq. (2);

$$L'_3 = L_3 \cos \phi + r_f \sin \phi \cdot \text{sign } \theta. \quad (2)$$

Taking into account Eq. (2), the overall equations of motion for the bicycle are given by Eqs. (3) - (5);

$$\dot{\psi} = V \frac{\tan \theta}{L_1 + L_2} \quad (3)$$

$$\begin{aligned} I_{xx} \ddot{\phi} = & I_{xz} \dot{\theta} \frac{V}{L(\cos^2 \theta)} + Mgh \sin \phi + Mh \frac{V^2 \tan \theta}{(L_1 + L_2)} \\ & + I_f \sec \theta \frac{V}{r_f} (\dot{\psi} + \dot{\theta}) + I_r (\dot{\psi}) \frac{V}{r_r} \\ & - Mg \frac{L_1}{L_1 + L_2} (L_3 \cos \phi + r_f \sin \phi \cdot \text{sign } \theta) \\ & \sin \theta \end{aligned} \quad (4)$$

$$\begin{aligned} I_h \ddot{\theta} = & -m_f g \sin(\phi - \theta \sin \lambda) f \\ & - I_f \cos \lambda \dot{\phi} \frac{V \tan \theta}{L_1 + L_2} + \tau_h - (c \dot{\theta} + d \text{sign } \dot{\theta}) \\ & - (L_3 \cos \phi + r_f \sin \phi \cdot \text{sign } \theta) \\ & \left\{ \frac{L_1 M g}{L_1 + L_2} \sin(\phi - \theta \sin \lambda) + \frac{L_1 M V^2}{(L_1 + L_2)^2} \sin \theta \right\}. \end{aligned} \quad (5)$$

In this study, the experimental validation is limited to a local stabilization problem, assuming that variations in the bicycle's roll angle remain small. However, future

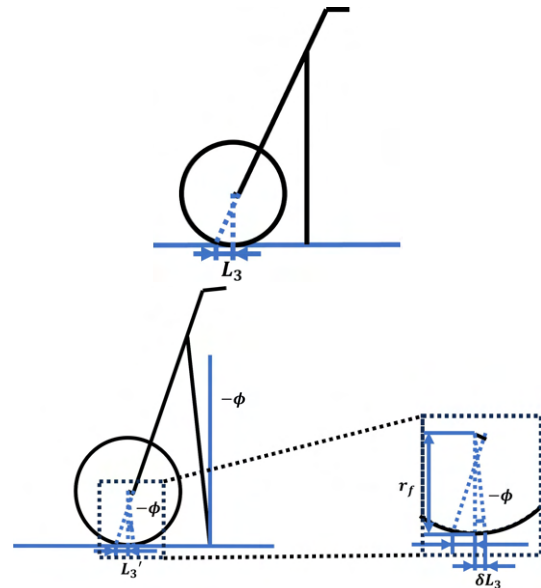


Fig. 2 Front wheel model

scenarios are expected to include situations in which the turning radius changes during motion. In such cases, it becomes necessary to consider the nonlinear coupling between the roll angle and steering angle, as well as nonlinearities arising from factors such as trail and the position of the center of mass. Compared to existing models, a distinctive feature of the proposed approach is that the complexity of these nonlinearities is constrained to a level that can be implemented on a microcontroller, taking into account computational load during controller implementation.

3. DESIGN OF POSTURE STABILIZATION CONTROL LAW

In this section, we calculate the equilibrium angle based on the equations of motion derived in Section 2, and design a posture stabilization control law around this equilibrium point.

3.1. Nonlinear Model

The behavior of a bicycle during turning while maintaining balance is regarded as an equilibrium state of the equations of motion. To achieve this, it is essential to derive a nonlinear state equation that reflects the bicycle's dynamics. When the input is defined as $u = [\tau_h, V^2]^T$ the state equation becomes Eq. (6);

$$\frac{d}{dt} \begin{bmatrix} \dot{\phi} \\ \dot{\theta} \\ \phi \\ \theta \\ \psi \end{bmatrix} = \begin{bmatrix} x_1 \\ x_2 \\ \dot{\phi} \\ \dot{\theta} \\ 0 \end{bmatrix} + \begin{bmatrix} 0 & y_1 \\ \frac{1}{I_h} & y_2 \\ 0 & 0 \\ 0 & 0 \\ 0 & y_5 \end{bmatrix} u. \quad (6)$$

Here, x_1 , x_2 , y_1 , y_2 , and y_5 can be expressed as follows.

$$\begin{aligned} x_1 &= \frac{Mgh \sin \phi}{I_{xx}} - Mg \frac{L_1}{(L_1 + L_2)I_{xx}} (L_3 \cos \phi + r_f \sin \phi \cdot \text{sign} \theta) \cdot \sin \theta \frac{I_{xz}}{I_{xx} L (\cos^2 \theta)} \dot{\theta} + \frac{MhV \tan \theta}{(L_1 + L_2)I_{xx}} + \frac{\dot{\theta}}{L (\cos^2 \theta)} + \frac{MhV \tan \theta}{(L_1 + L_2)I_{xx}} + \frac{I_f \sec \theta (\dot{\psi} + \dot{\theta})}{r_f \cdot I_{xx}} + \frac{I_r (\dot{\psi})}{r_r \cdot I_{xx}} \\ x_2 &= \frac{-m_f g \sin(\phi - \theta \sin \lambda) f}{I_h} - \frac{(c\dot{\theta} + d \text{sign} \dot{\theta})}{I_h} - \frac{(L_3 \cos \phi + r_f \sin \phi \cdot \text{sign} \theta)}{I_h} \cdot \frac{L_1 Mg}{L_1 + L_2} \sin(\phi - \theta \sin \lambda) \\ y_1 &= \frac{I_{xz}}{I_{xx} L (\cos^2 \theta)} \dot{\theta} + \frac{MhV \tan \theta}{(L_1 + L_2)I_{xx}} + \frac{I_f \sec \theta (\dot{\psi} + \dot{\theta})}{r_f \cdot I_{xx}} + \frac{I_r \dot{\psi}}{r_r \cdot I_{xx}} \end{aligned}$$

$$\begin{aligned} y_2 &= -I_f \cos \lambda \dot{\phi} \frac{1}{r_r I_h} - \frac{(L_3 \cos \phi + r_f \sin \phi \cdot \text{sign} \theta)}{I_h} \cdot \frac{L_1 MV}{(L_1 + L_2)^2} \sin \theta \\ y_5 &= \frac{\tan \theta}{L_1 + L_2}. \end{aligned} \quad (7)$$

3.2. Equilibrium Analysis

We consider the situation in which a bicycle is turning while in a state of equilibrium. The equilibrium state is defined as the condition in which the system's state variables remain at their equilibrium values. In order for the bicycle to maintain equilibrium while in motion, the centrifugal force and gravitational force must be balanced, as shown in Fig. 3. Under this condition, the velocity is derived from the equations of motion of the bicycle, and a control law is designed to maintain the equilibrium state.

As an example, we derive the velocity required to maintain a turning radius of 5 m and a roll angle of -5 degrees. The steering angle can be calculated from the turning radius b_r using Eq. (8);

$$\begin{aligned} \tan \theta &= \frac{L_1 + L_2}{b_r} \\ \theta &= \tan^{-1} \left(\frac{L_1 + L_2}{b_r} \right) \\ &= 0.2431 \text{ rad}. \end{aligned} \quad (8)$$

Furthermore, since the roll angle and steering angle of the bicycle do not deviate from their equilibrium values, the roll angular acceleration and steering angular velocity are zero. Therefore, the velocity required to maintain the equilibrium state is given by Eq. (9);

$$\begin{aligned} V^2 &= (-Mgh \sin \phi + Mg \frac{L_1}{L_1 + L_2} (L_3 \cos \phi + r_f \sin \phi \cdot \text{sign} \theta)) / (Mh \frac{\tan \theta}{(L_1 + L_2)} + I_f \sec \theta \frac{1}{b_r} + I_r \frac{1}{b_r r_r}) \\ V &= 2.02085 \text{ m/s}. \end{aligned} \quad (9)$$

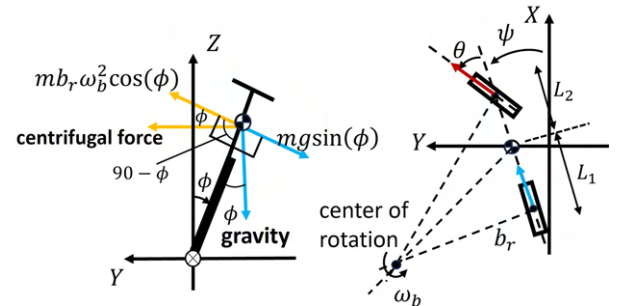


Fig. 3 Bicycle model when gravity and centrifugal force are balanced

4. HARDWARE IMPLEMENTATION AND EXPERIMENTAL VERIFICATION

We propose a speed-assist control method to maintain the equilibrium state of a bicycle and verify its effectiveness through driving experiments.

4.1. System Configuration

The configuration diagram of the bicycle experimental setup used in this study is shown in Fig. 4, and the physical parameters are listed in Table 2. A motor with an encoder mounted on the handlebar assists in steering torque and measures the handlebar angle. An IMU installed at the rear of the saddle measures 3-axis angles and angular velocities. A hall sensor mounted on the rear wheel measures the vehicle speed. Additionally, a motor linked to the pedal crank axis can drive the rear wheel to assist the rider's pedaling.

4.2. Speed Control

The block diagram of the speed-assist control implemented on the bicycle is shown in Fig. 5. The speed input derived in Section 3 represents the velocity required to maintain the roll angle in the equilibrium state. However, since a rider cannot always maintain the equilibrium

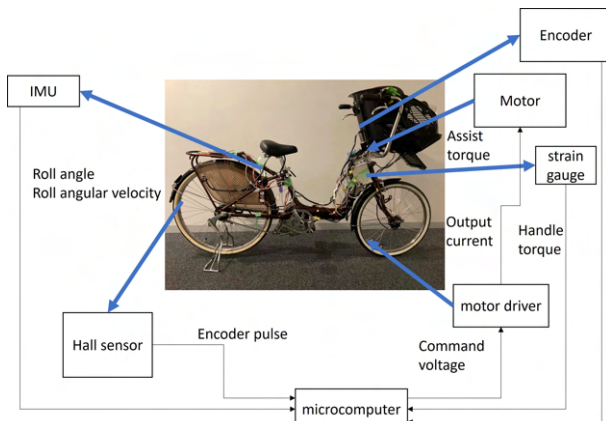


Fig. 4 System Configuration

Table 2 Physical parameters of experimental system

symbol	description
M	29.8 kg
m_f	2.00 kg
L	1.24 m
L_1	0.5243 m
L_2	0.7157 m
L_3	0.0532 m
h	0.41607 m
f	0.05 m
r_f	0.28 m
r_r	0.33 m
λ	0.35 rad
I_{xx}	9.8 kgm ²
I_{xz}	4.411 kgm ²
I_h	0.878 kgm ²
I_f	0.156 kgm ²
I_{rf}	0.304 kgm ²
c	0.2186
d	2.344

state during riding, a control system is designed to adjust the target speed based on the bicycle's roll angular velocity. With this control, even if the handlebar angle or roll angle deviates from the ideal equilibrium state due to human operation, the system automatically adjusts to the speed corresponding to the new equilibrium condition, thereby achieving stable riding. The target vehicle speed in the designed control system is determined using the roll angular velocity gain α and is given by Eq. (10);

$$V = V_0 + \alpha \dot{\phi}. \quad (10)$$

4.3. Riding Experiment

To evaluate the effectiveness of the proposed control law, three experiments were conducted. In the first experiment, no control is applied; the rider rides along a constant turning radius relying solely on their own control. In the second experiment, the handlebar angle is fixed using the handlebar-assist motor, and the pedal motor is controlled to achieve the equilibrium speed. This simulates the behavior of a rider who cannot maintain stable riding. Here, the reason for using the handlebar-assist motor is not to assist with steering operation but to fix the handlebar angle at a constant value to simulate it. In the third experiment, the proposed speed-assist control is implemented to enhance stable riding even when the handlebar angle is fixed, in order to simulate the same unstable riding condition as in the second experiment.

The turning path used in the experiment is shown in Fig. 6. Cone markers were placed at 45-degree intervals along a circle with a radius of 5 meters. To prevent deviation from the turning radius, additional cone markers were placed at the 6-meter radius in the same interval, and the bicycle was ridden between these markers. Fig. 7 illustrates the experimental scene in progress.

In the riding experiments, a male participant in his 20s rode the bicycle twice along the path shown in Fig. 6. The characteristics of the bicycle's riding trajectory are also shown in Fig. 8. Because the experiment site included elevation changes, the riding path involved three sections: flat, uphill and downhill, as illustrated in Fig. 8.

4.4. Experimental Results

Since the bicycle becomes more susceptible to wobbling as its speed decreases, we analyze the data collected

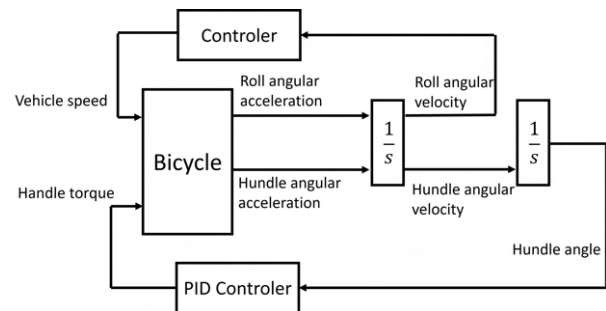


Fig. 5 Block diagram of the proposed speed-assist control

while the bicycle is ascending a slope. Figs. 9 – 14 show the results for three conditions: (A) no control applied, with only manual rider input to maintain a handlebar angle of 14 degrees, a roll angle of -5 degrees, and a target turning radius of 5m; (B) fixed handlebar angle with the pedal motor controlled to achieve the velocity corresponding to the equilibrium point; and (C) fixed handlebar angle with the proposed-assist control implemented.

Each graph displays data from six trials, with each trial distinguished by a different color: blue (1st), orange (2nd), yellow (3rd), purple (4th), green (5th), and light blue (6th). The vertical axes of the graphs represent roll angular acceleration and roll angular velocity, while the horizontal axis indicates the yaw angle over the slope-climbing section. The standard deviations of each conditions are summarized in Table 3.

First, we analyze the behavior when the rider is unable to ride the bicycle properly. Comparing the roll angular velocity in Condition A and B, the standard deviations are 2.1800 and 3.1431, respectively, indicating greater rider body vibration in Condition B, unstable riding case. This vibration appears to result from large fluctuations in roll angular acceleration, suggesting that destabilizing forces are acting in the direction of falling. Therefore, the speed-assist control is necessary to suppress such vibrations.

Next, when Condition B and C, comparing the roll angular acceleration between the case where the rider cannot ride properly and the case it is confirmed that the proposed method successfully suppresses the vibrations. The standard deviations are 0.2932 and 0.1982, respectively, indicating reduced variability and suppression of destabilizing forces. Similarly, when comparing the roll angular velocity between Condition B and C, the standard deviations are 3.1431 and 2.1978, respectively. These results show that suppressing falling-direction forces reduces body vibration. Overall, these findings verify that the proposed speed-assist control is effective in stabilizing the posture of the bicycle.

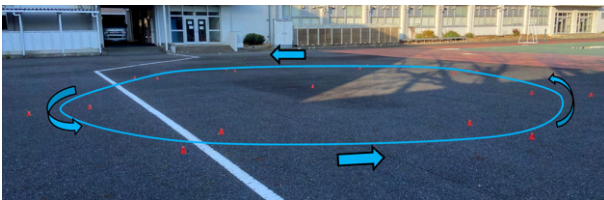


Fig. 6 Test Course for Riding Experiments



Fig. 7 Scene from the Riding Experiment

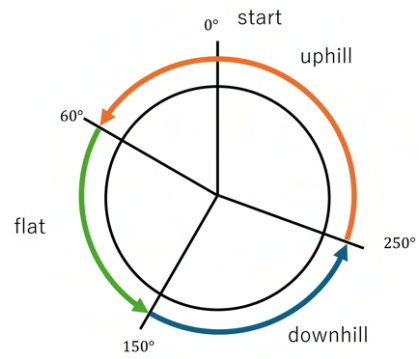


Fig. 8 Driving path environment

5. CONCLUSION

In this study, we proposed a speed-assist control method to enhance riding stability, even when the bicycle's balance is compromised due to inappropriate rider

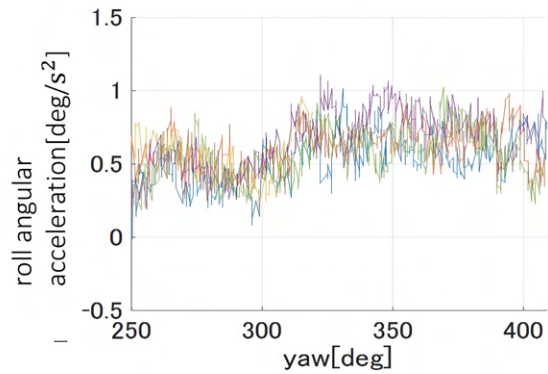


Fig. 9 Roll angular acceleration in Condition A

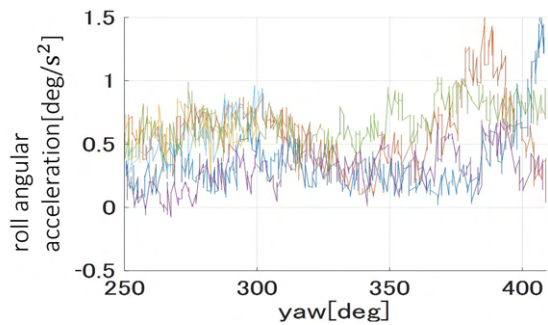


Fig. 10 Roll angular acceleration in Condition B

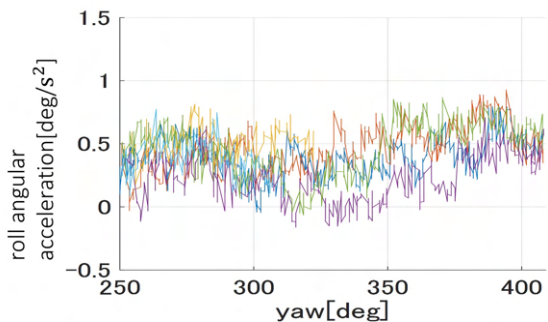


Fig. 11 Roll angular acceleration in Condition C

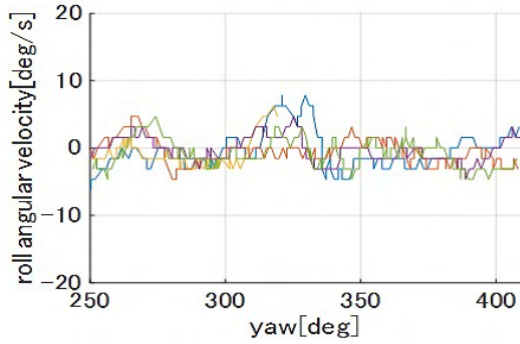


Fig. 12 Roll angular velocity in Condition A

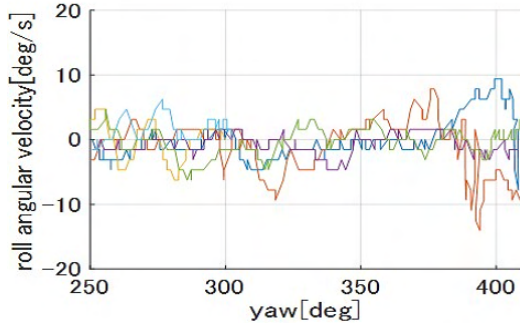


Fig. 13 Roll angular velocity in Condition B

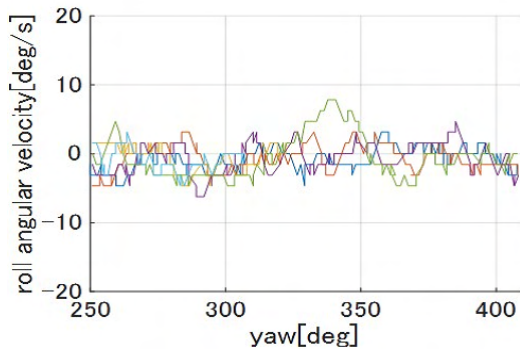


Fig. 14 Roll angular velocity in Condition C

Table 3 Standard deviation for each condition

	roll angular acceleration	roll angular velocity
ConditionA	0.1763	2.1800
ConditionB	0.2932	3.1431
ConditionC	0.1982	2.1978

operation. To develop this control system, the mathematical bicycle model was derived, and the equilibrium points of the motion were identified. Based on this analysis, the speed-assist control was designed to maintain stable riding along a specified turning radius. The experimental results demonstrated that the proposed control, derived from the equilibrium point analysis, is effective in stabilizing the bicycle's posture.

In future work, we plan to verify through mathematical simulations and real-world implementation whether the system can adapt to changes in the turning radius when the equilibrium point shifts. It should be noted that the experiments conducted in this study were real-

world tests with dynamic rider input, not simply physical tests under idealized conditions. The control system is intended to handle general balance disturbances, not only those caused by inappropriate operation.

6. ACKNOWLEDGMENT

This study was partially supported by JSPS KAKENHI Grant Number 24K01008.

REFERENCES

- [1] Oliver O'Brien, James Cheshire, Michael Batty, "Mining bicycle sharing data for generating insights into sustainable transport systems", *Journal of Transport Geography*, Vol. 34, pp. 262–273, 2014.
- [2] Lishuang Bian, Qizhou Hu, Xin Zhang, Xiaoyu Wu, Minjia Tan, "Dynamic Investigations of Shared Bicycle Operators' Competition Based on Profit Maximization", *Appl. Sci.* 2024, 14(20), 9223, 2014.
- [3] Yongping Zhang, Zhifu Mi, "Environmental benefits of bike sharing: A big data-based analysis", *applied Energy*, Vol. 220, pp. 296–301, 2018.
- [4] Xiaozhou Ye, "Bike-Sharing Adoption in Cross-National Contexts: An Empirical Research on the Factors Affecting Users' Intentions", *Sustainability* 2022, 14(6), 3208, 2022.
- [5] Arend L Schwab, J. P. Meijaard, "A review on bicycle dynamics and rider control", *Vehicle System Dynamics*, Vol. 51, No. 7, pp. 1059–1090, 2013.
- [6] Chin-Keng CHEN, Thanh-Son DAO, "Genetic fuzzy control for path-tracking of an autonomous robotic bicycle", *Journal of System Design and Dynamics*, Vol. 1, No. 3, 2007.
- [7] Ronald Smith, Ziad Fawaz, Alireza Mohammadi, Paul Muench, Sridhar Lakshmanan, "Linear parameter varying based control of a riderless bicycle with linear actuators", *Proceedings of the SPIE*, Vol. 110210, 110210C7, 2019.
- [8] Yasuhito Tanaka, Toshiyuki Murakami, "Self sustaining bicycle robot with steering controller", *The 8th IEEE International Workshop on Advanced Motion Control 2004*, pp. 148–151, 2004.
- [9] Lychee Keo, Sirichai Pornsarayouth, Masaki Yamakita, Kazuhiro Ito, "Stabilization of an Unmanned Bicycle with Flywheel Balancer", *IFAC Proceedings Volumes*, Vol. 43, Issue 14, pp. 475–480, 2010.
- [10] Pongsakorn Seekhao, Kanokvate Tungpimolrut, Manukid Parnichkun, "Development and control of a bicycle robot based on steering and pendulum balancing", *Mechatronics*, vol. 69, 102386, 2020.
- [11] Tim Jones, Lucas Harms, Eva Heinen, "Motives, perceptions and experiences of electric bicycle owners and implications for health, wellbeing and mobility", *Journal of Transport Geography*, vol. 53, pp. 41–49, 2016.
- [12] Karl J. Åström, R.E. Klein, A. Lennartsson, "Bicycle dynamics and control: adapted bicycles for education and research", *JIEEE Control Systems Magazine*, vol. 25, No. 4, pp. 26–47, 2005.